Neuroscience Vol. 51, No. 2, pp. 445–450, 1992
Printed in Great Britain

0306-4522/92 \$5.00 + 0.00
Pergamon Press Ltd

DYNAMICS OF RESPONSES OF V1 NEURONS EVOKED BY STIMULATION OF DIFFERENT ZONES OF RECEPTIVE FIELD

I. A. Shevelev,* M. A. Volgushev and G. A. Sharaev

Laboratory of Sensory Systems, Institute of Higher Nervous Activity and Neurophysiology,
Russian Academy of Sciences, 5a Butlerova str., GSP-7, Moscow 117865, Russia

Abstract—The dynamics of receptive fields of 73 neurons in area 17 of cat visual cortex were studied using the temporal slice method. Three-dimensional maps of the receptive fields were plotted using the criterion of spike number in successive fragments (step 10 or 20 ms) of responses to 100 local flashes presented at different parts of the receptive field in random order. The size and configuration of such dynamically recorded receptive fields were then estimated. This allowed us to reveal the dynamic reorganization of all receptive fields 20–400 ms after stimulation. A small zone of responses appeared in the receptive field after initial latency, then it widened, received definitive configuration, and after that decreased and disappeared. The effect was reproducible under repeated estimations.

The relationships between receptive field and the previously described orientation tuning dynamics, as well as between dynamics of receptive fields and their summation zones, mechanisms and possible functional meaning of the revealed effects for signal processing in the primary visual cortex are discussed.

Previously, deep reorganization of the classical[7,8] receptive fields (RF) of cat cortical units with a change in light background level,[1,16–19,22,28–30,34] as well as following the change in alertness level[1,9,11,12,15,19,27,33] were found. These adaptive reorganizations of RF normally occur within seconds or dozens of seconds. There is a line of evidence that there exists dynamic readjustment of RF properties,[5,6,12,14,18,19,30,35–37] which occurs within tens of milliseconds after stimulus onset and could be important for visual information processing in the cerebral cortex.

The main aim of our study was to find fast RF dynamics and to estimate some characteristics of the process. We analysed neuronal responses using the temporal slice method previously used for estimation of spatial summation in the LGB units.[14]

EXPERIMENTAL PROCEDURES

Animals, narcosis and surgery

Adult cats of standard weight (2.7–3.3 kg) were anaesthetized by ether for usual surgery. These animals were kept under Sombrevin (5% solution, 3–5 mg/kg, i.v.) or under Nembuthal (5% solution, 30 mg/kg, i.p.) anaesthesia and were immobilized with D-tubocurarine (0.15 mg/kg, 10% solution). Experiments began 3–4 h after ether action. The animals were intubated and kept on artificial respiration and their rectal temperature was kept constant by body thermostabilization. Blood pressure, pulse rate and body temperature were monitored and kept within normal limits. The state of the cerebral cortex was monitored by electroencephalogram.

The third eyelid of the right eye was contracted by Neo-Synephrine and the eyelids opened; a contact lens (0 D) was put on the eye (artificial pupil diameter 3 mm), and a correcting lens matched by projectional ophthalmoscopy[4] was placed in front of the eye. The pupil size was stabilized with 0.1% Atropin solution, and the left eye was covered with an opaque partition.

The skull was trephined over area 17 of the visual cortex (VC): P0.5–3; L0.5–2 mm. The cat's head was fixed with a metal platform previously attached to the skull.

Recording

The microelectrodes were either glass micropipettes filled with 2.5 M NaCl solution with a resistance of 5–15 MΩ at a frequency of 60 Hz, or acetate-coated tungsten wires with a resistance of 1–5 MΩ. Extracellularly recorded impulses from 73 single units of the left area 17 of the VC contralateral to the stimulated eye were fed to a threshold discriminator and then onto a computer.

Light stimulation

The experiments were carried out in a light- and sound-proof chamber under background illuminations of 0.1, 0.84 and 3.0 cd/m^2 and stimuli contrasts 7×10^{-6}–7×10^{2}. For RF mapping, 100 (10 × 10) flashes of round or rectangular light spots were presented in a randomized order in the part of the visual field containing RF. The search of RF and its detailed study were performed by computer-controlled projection of the moving or flashing stimuli[19] to a white reflecting screen (62 × 65°, 1.7 m from the eye; $K_r = 0.89$). The stimulus size varied from 0.25° to 4°; it was presented on 5–400 ms at the rate of 0.5 s^{-1}. The duration of one testing of RF was equal to 3.3 min; this procedure was usually repeated 2–10 times. Stimuli were viewed monocularly by the right eye contralateral to the left hemisphere, from which the activity was derived.

Processing

For each position of the light spot in the RF, 2–10 responses were collected by the computer for peristimulus–time histograms (PSTHs). PSTHs were processed by a temporal slice method.[14] This means that we estimated the RF of a cortical unit by the number of discharges in successive time fragments or portions of responses, instead

---

*To whom correspondence should be addressed.

Abbreviations: PSTH, peristimulus–time histogram; RF, receptive field; VC, visual cortex.

of a total number or maximal instantaneous frequency of impulses in a reaction. The set of the RF three-dimensional maps was plotted by computer. The first such map was plotted for the first 20 ms after the stimulus, the second for the next 20 ms, and so on (differential slices of RF). RF size and configuration were estimated in each of these maps.

Repeated measurements of RF characteristics under the same conditions at the same unit allowed us to estimate the reproducibility of our data; their reliability was assessed using standard statistical criteria.

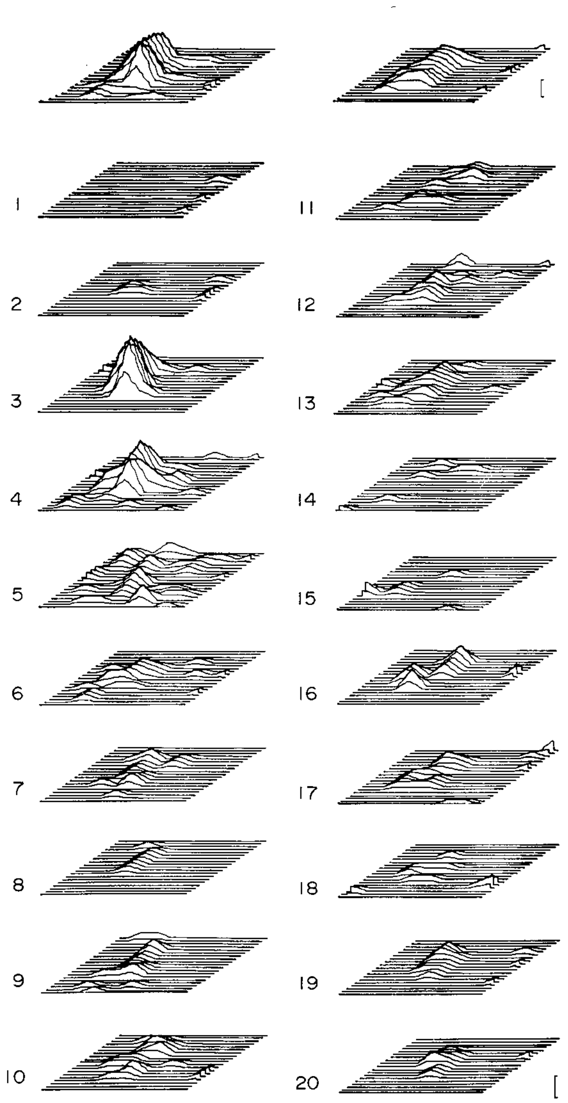

Fig. 1. Dynamics of recorded excitatory on- and off-zone of the neuron RF in the cat visual cortex. The upper maps in each column correspond to the RF plot by the total number of spikes during 200 ms of the on-response (left) and 200 ms of the off-response (right). The stimulus was a light square (1 × 1°), flashed in randomized order in 100 (10 × 10) parts of the visual field tested area (11 × 11° at 11° from the field centre) in the mesopic condition. The horizontal axis of the map corresponds to the screen vertical, while the second axis is its horizontal dimension. On the vertical axis of the map the number of spikes during 200 ms are shown. Calibration (upper): 10 spikes/200 ms. Maps 1–20 are plotted by successive 20 ms fragments of the unit responses; maps 1–10 correspond to the on-responses, while maps 11–20 are the off-responses. Calibration (lower): 5 spikes/20 ms.

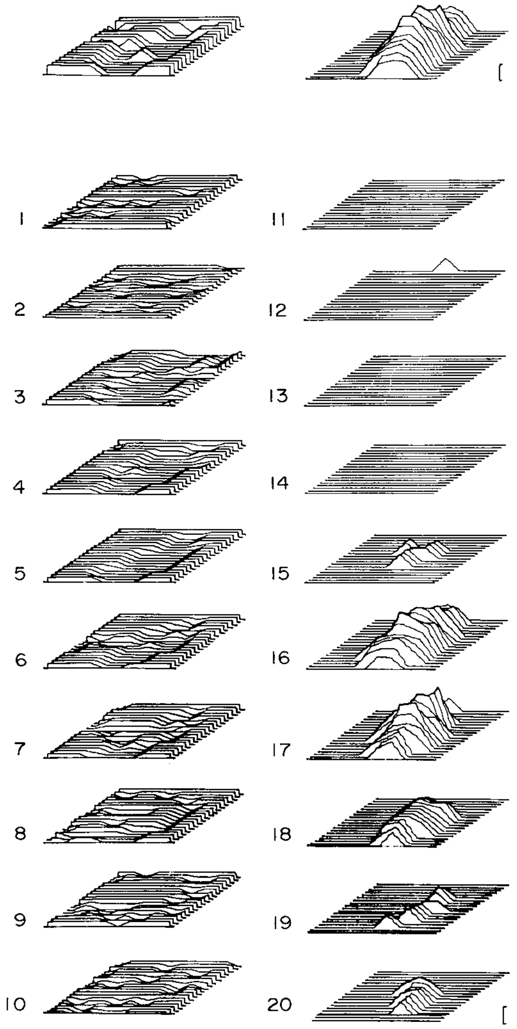

Fig. 2. RF dynamics of the unit with inhibitory on-responses (left column) and excitatory off-responses (right column). In the on-maps for the clear demonstration of the inhibitory zone of the RF the background activity and excitatory responses are equalized. The stimulus was a light square (0.5 × 0.5°) flashed in 100 visual field points (area 7 × 4° at 12° from the centre of the visual field); mesopic adaptation. Calibration: 25 spikes/200 ms (upper two maps) and 10 spikes/20 ms (maps 1–20). Other details as in Fig. 1.

RESULTS

Examples of dynamics of the recorded receptive field

All 73 studied neurons of the visual cortex revealed similar fast reorganization of the recorded RF during generation of their responses to local testing light flashes. Typically, recorded RF after initial latency was small and weak and appeared only in the central part of the tested area (Fig. 1, map 2). This zone successively widened, discharge numbers increased (maps 3–5) and then the RF relief narrowed and weakened (maps 6–8). In many cases at the end of on- or off-responses, recorded RF even disappeared or was separated into small fragments. Figure 1 illustrates that when the second phase of the excitatory on-responses was generated secondary widening was

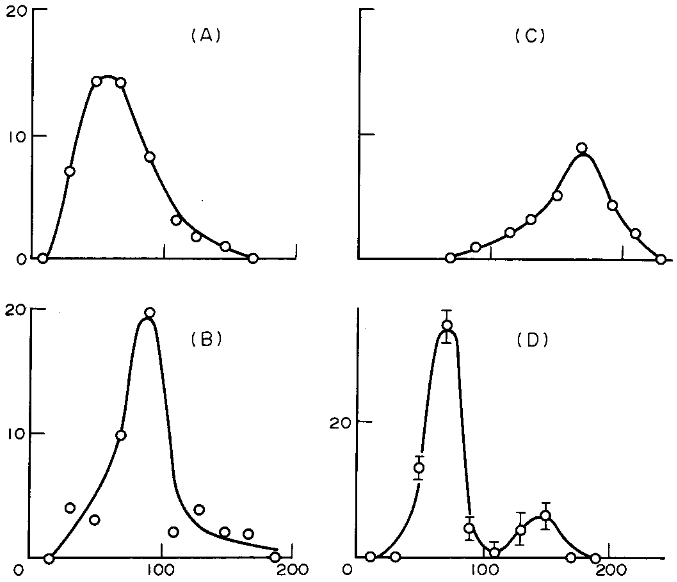

Fig. 3. Distribution of neurons in the visual cortex by the temporal characteristics of RF dynamics (A–C) and its stability (D). (A) Distribution of initial latency of dynamically recorded RF appearance. (B) Distribution of the moments of RF maximal widening. (C) Distribution of the moment of disappearance of recorded RF. Abscissa: time after stimuli onset, ms; ordinate: number of neurons ($n = 29$ for A, 47 for B and 26 for C). Abscissae in A and C correspond to abscissae in B and D. Ordinate in C corresponds to ordinate in A. (D) RF area in typical neuron (ordinate in deg^2) vs time after stimulus onset (abscissa in ms). Mean data and their errors are shown for five successive estimations of the RF dynamics.

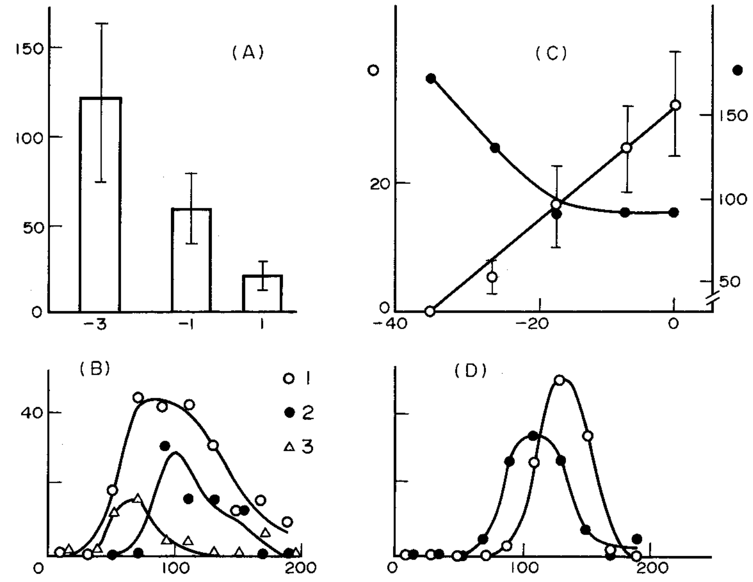

Fig. 4. Maximal receptive field area under dynamic estimation as a function of the background illumination with constant test intensity (A), with constant test contrast (B) and as a function of intensity (C), and of energy of the testing flash (D). (A) Mean RF area and S.E. for 20 neurons (ordinate, deg^2) vs background illumination of the screen (abscissa, log of lux). (B) The RF area (ordinate, deg^2) vs time after test stimulus onset (abscissa, ms) under different stimuli/background contrast (1 and 2; 1 and 3) and equal contrast (2 and 3). (1) Stimuli intensity 70 lux on background 0.1 lux ($C = 700$); (2) 0.7 lux on 0.1 lux ($C = 7$); (3) 70 lux on 10 lux ($C = 7$). (C) The RF area (ordinate, relative units; mean data and their S.E. for 17 neurons) vs stimuli intensity (abscissa, dB of light attenuation; 0 dB corresponds to 70 lux). (1) RF area, (2) peak latency of RF maximal dynamical widening. (D) The RF area (ordinate, deg^2) vs time after stimulus onset (abscissa, ms) under testing of RF with flashes of equal energy. (1) stimulus 1 × 1°, intensity 35 lux; (2) stimulus 0.5 × 1°, intensity 70 lux.

reflected in RF (maps 9–11) and partial masking of the latency and early phase of the off-responses was seen (maps 11–13).

The same dynamics of RF were revealed during off-response generation (Fig. 1, maps 11-20) and in the cases where RFs had a central inhibitory on-zone in their RF (Fig. 2).

The RF configuration became definitive (typically of prolonged form) at early stages of its dynamics (Figs 1 and 2) and remained up to the recorded field fragmentation and disappearance.

Statistical characteristics of receptive field dynamics

The described effect was highly reproducible: it may be revealed many times under successive testing with small variations (Fig. 3D). The recorded RF appeared in different units at 20–100 ms after the onset of testing flashes (Fig. 3A, mode on 60 ms), became maximal (10–220 deg^2 under mesopic conditions) at 40–140 ms (B, mode on 90 ms), and disappeared at 120–220 ms (C, mode on 170 ms).

We could not obtain reliable differences in the RF dynamics for simple, complex and hypercomplex fields.

Dependence of receptive field dynamics on the parameters of the testing light

The size of the recorded RF was inverse proportional to the background light level in conditions of equal intensity (Fig. 4A), as well as of equal contrast testing (Fig. 4B). It is seen (Fig. 4A) that under transition from low scotopic to mesopic and then to photopic background levels, dynamically recorded RFs decreased in size (by 2.3 and 6 times, respectively). It is interesting that these pronounced changes of RF size were not followed by changes in temporal characteristics of RF dynamics: the peak latency of the process in these conditions varied by only 5% (Fig. 4B, 1 and 3). Under equal contrast testing (Fig. 4B, 2 and 3) RF in two-thirds of cases decreased with the rise of the light background. However, the latency in such cases reliably shortened. The same was true for test flashes of equal energy, but different size and intensity (Fig. 4D).

RF dynamics depended on the test stimulus intensity or contrast level (Fig. 4C, 1). Overall RF size as well as its maximal widening during dynamics were directly connected with these parameters, while initial and peak latencies of the process shortened with increased intensity (Fig. 4C, 2). Similar relations were revealed between the characteristics of RF dynamics and test flash size (Fig. 5A), while for flash duration (Fig. 5B) and orientation (Fig. 5C) these relations looked more complex. Thus, under flash prolongation, after individually varied critical duration (from 5 to 100 ms in different neurons, modal estimate 25 ms) the RF widening was changed by its

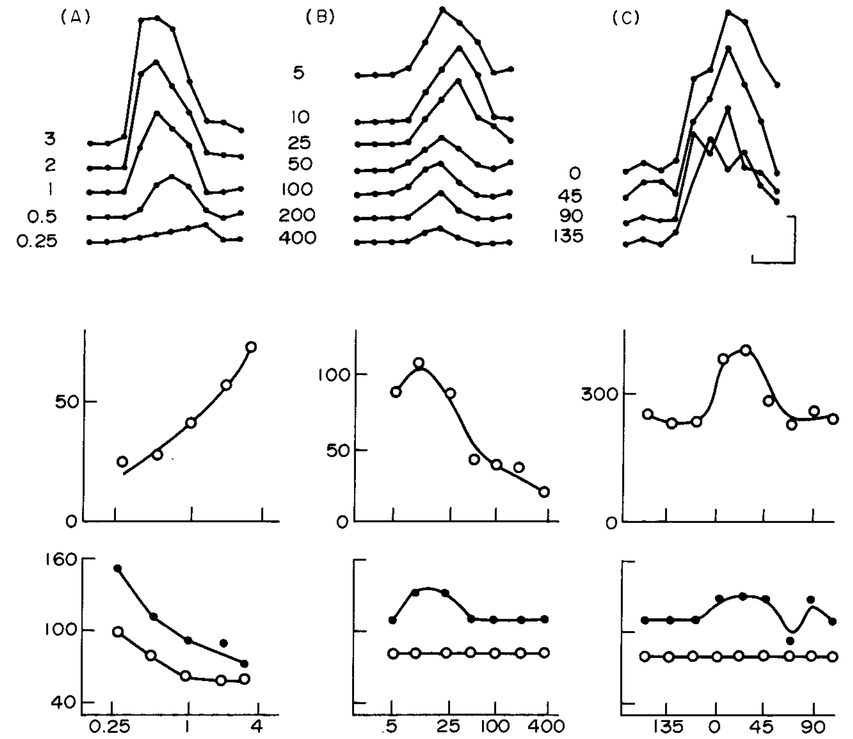

Fig. 5. Maximal receptive field area under dynamic estimation and temporal characteristics of these dynamics as a function of the test stimulus size (A), duration (B) and orientation (C). Upper row: dynamics of RF area under different parameters of the stimuli, shown at the left of each curve in deg (A), ms (B) and deg (C). Middle row: RF area (ordinate, deg^2) vs stimuli parameters. Lower row: latencies of the RF development in dynamics (ordinate, ms; white dots—initial latency, black dots—peak latency) vs stimuli parameters.

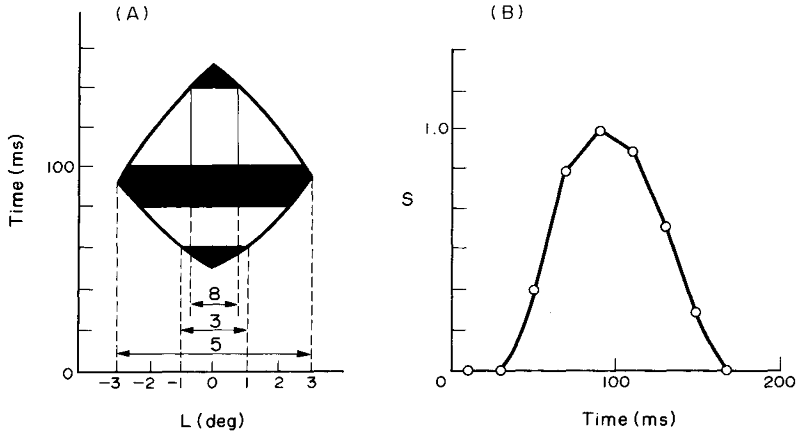

Fig. 6. (A) Scheme of dependence of the temporal characteristics of response of the visual cortex neuron on the testing light spot position in the receptive field. Abscissa: distance of the test flash from the RF centre (0°), deg; ordinate: initial latency of the unit response (lower curve) and time of the discharge cessation (upper curve), ms; figures 3, 5 and 8 inside the panel show the RF diameter at appropriate slices (black end). (B) Dynamics of this receptive field area. Abscissa: time after stimuli onset, ms; ordinate: area of the RF, relative units.

decay (Fig. 5B). Dynamically estimated RF size revealed typical orientation tuning (Fig. 5C) that coincided with standard estimations of this function.

DISCUSSION

At least three issues must be discussed here: whether the revealed effect is an artifact, what can be its neurophysiological mechanisms and what is its functional meaning?

Are the receptive field dynamics an artifact?

The existence of RF dynamics in all units under study, their reproducibility under different stimuli parameters and under repeated estimations indicates the objective, non-incident nature of the described phenomenon. We can conclude that it is not an artifact.

Neurophysiological mechanism of receptive field dynamics

The dynamics of the recorded RF evidently depend, first of all, on the different temporal course of the unit's excitation evoked by the local light testing at different parts of the RF (Fig. 6). Different weights of inputs at these locations lead to a change in response pattern, which is demonstrated schematically in Fig. 6. While under local flash stimulation at the centre of the RF the unit generates short-latency and prolonged discharges, the response under testing of the RF periphery is long-latency and short one. This shortening of the response is connected both with lower weight of excitatory inputs and with relatively stronger inhibition at the RF periphery.[2,3,17–20,28,29,31,32,34] The above-mentioned changes of response characteristics are evident from the results described above. They are necessary and sufficient for the explanation of RF dynamics in the majority of units. It should be noted that in some rare cases the responses from the central zone of RF demonstrated relatively fast successive inhibition after initial discharge. Then an inhibitory hole at the centre of the circular excitatory zone is recorded at certain times during the RF dynamics. However, as a rule, small local flashes are not sufficient enough for the effective activation of the relatively high-threshold[15,25] inhibitory mechanisms of the RF.

Functional meaning of the receptive field dynamics

This problem can only be discussed speculatively. Really, as in any other case of neural events, we cannot obtain proof of its non-epiphenomenal nature, only of the real significance for the next neuron-recipient of the message.[13] Nevertheless, it seems tempting to consider different dynamics of excitatory and inhibitory zones in RF as a source of a special type of orientation tuning dynamics that we described previously.[15,21,23–26] It was shown that two-thirds of cortical units dynamically retuned their preferred orientation within some part of the orientation range during the response generation. Such "scanners" can play an important role in the spatiotemporal orientation coding that we suggested.[15,21,23–26] It is especially interesting that the time of RF dynamic widening demonstrated here coincides with: (i) the time of dynamic orientation tuning widening in the majority of cells,[19,21] and (ii) the time of the drop of human orientation recognition probability.[10] The second probable usage of RF dynamics at the LGB level was supposed by Podvigin,[14] who believed that the LGB units with such properties of their RFs can be retuned filters of the spatial frequencies.

REFERENCES

1. Bear D. M., Sasaki H. and Ervin F. R. (1971) Sequential change in receptive fields of striate neurons in dark adapted cats. *Expl Brain Res.* **13,** 256–272.
2. Benevento L. A., Creutzfeldt O. D. and Kuhnt U. (1972) Significance of intracortical inhibition in the visual cortex. *Nature New Biol.* **238,** 124–126.
3. Creutzfeldt O. D., Kuhnt U. and Benevento L. A. (1974) An intracellular analysis of visual cortical neurones to moving stimuli: responses in a co-operative neuronal network. *Expl Brain Res.* **21,** 251–274.
4. Fernald R. and Chase R. (1971) An improved method for plotting retinal landmarks and focusing the eyes. *Vis. Res.* **11,** 95–96.
5. Fries W. and Albus L. (1976) Static and dynamic properties of receptive fields of some simple cells in cat's striate cortex. *Vis. Res.* **16,** 563–566.
6. Hida E. and Naka K.-I. (1982) Spatio-temporal receptive fields as revealed by spatio-temporal random noise. *Z. Naturforsch.* **37c,** 1048–1049.
7. Hubel D. H. and Wiesel T. N. (1962) Receptive fields, binocular interaction and functional architecture in the cat's visual cortex. *J. Physiol., Lond.* **160,** 106–154.
8. Hubel D. H. and Wiesel T. N. (1965) Receptive fields and functional architecture in two non-striate visual areas (18 and 19) of the cat. *J. Neurophysiol.* **28,** 229–289.
9. Ikeda H. and Wright M. J. (1974) Sensitivity of neurones in visual cortex (area 17) under different levels of anaesthesia. *Expl Brain Res.* **20,** 471–484.
10. Kostelianez N. B. and Kamenkovich V. M. (1982) Dynamics of the process of orientation estimation in human. *Physiologia Cheloveka, Moscow* **8,** 559–563 [in Russian].
11. Lee B. B. (1970) Effect of anaesthetics upon visual responses in the cat's striate cortex. *J. Physiol., Lond.* **207,** 74P.
12. Luhmann H. J., Greuel J. M. and Singer W. (1990) Horizontal interactions in cat striate cortex. 3. Ectopic receptive fields and transient exuberance of tangential interactions. *Eur. J. Neurosci.* **2,** 369–377.
13. Perkel D. H. and Bullock T. H. (1969) Neural coding. *Neurosci. Res. Symp. Summ.* **6,** 405–527.
14. Podvigin N. F. (1979) *Dynamic Properties of Neuronal Structures of the Visual System.* Nauka, Leningrad [in Russian].
15. Robertson A. D. J. (1965) Anaesthesia and receptive fields. *Nature, Lond.* **205,** 80P.
16. Sasaki H., Saito Y., Bear D. M. and Ervin F. R. (1971) Quantitative variation in striate receptive fields of cats as a function of light and dark adaptation. *Expl Brain Res.* **13,** 273–293.
17. Shevelev I. A. (1977) Plasticity of specialized detector properties of neurons of the visual cortex. In *Sensory Systems,* pp. 20–36. Nauka, Leningrad [in Russian].
18. Shevelev I. A. (1982) *Adaptivity and Dynamic Properties of Visual Cortex Neurons,* pp. 76–96. Mir, Moscow.
19. Shevelev I. A. (1984) *Neurons of the Visual Cortex: Adaptivity and Dynamics of Receptive Fields.* Nauka, Moscow [in Russian].
20. Shevelev I. A. (1985) Basic mechanisms of visual cortex inhibition. *Physiol. J., Kiev* **31,** 562–569 [in Russian].
21. Shevelev I. A., Lazareva N. A., Novikova R. V., Sharaev G. A. and Tichomirov A. S. (1987) Orientation scanning effect monitored in neurons of the cat visual cortex. *Neurophysiologia, Kiev* **19,** 138–142 [in Russian].
22. Shevelev I. A. and Maksimova I. V. (1979) Adaptivity of receptive fields of neurons in the visual cortex. In *Sensory Systems,* pp. 62–78. Nauka, Leningrad [in Russian].
23. Shevelev I. A. and Sharaev G. A. (1981) Scanning of orientational range by the neurones of the cat visual cortex. *Dokl. Acad. Nauk SSSR* **256,** 1506–1509 [in Russian].
24. Shevelev I. A. and Sharaev G. A. (1981) Dynamics of orientational tuning of units in the cat visual cortex. *Neurophysiologia, Kiev* **13,** 451–459 [in Russian].
25. Shevelev I. A. and Sharaev G. A. (1982) Dynamics of orientational tuning of units in the cat visual cortex. *Neuroscience* **8,** Suppl., 192.
26. Shevelev I. A. and Sharaev G. A. (1985) Timers and scanners among the orientation detectors in the cat visual cortex. *Neurophysiologia, Kiev* **17,** 35–43 [in Russian].
27. Shevelev I. A. and Verderevskaja N. N. (1982) Receptive fields of neurons in the cat visual cortex under changes in alertness level. In *Sensory Systems,* pp. 41–54. Nauka, Leningrad [in Russian].
28. Shevelev I. A., Verderevskaja N. N. and Marchenko V. G. (1984) Complete reorganization of detector properties of neurons in the cat visual cortex under different levels of visual adaptation. *Dokl. Acad. Nauk SSSR* **217,** 493–496 [in Russian].
29. Shevelev I. A., Verderevskaja N. N., Marchenko V. G. and Maksimova I. V. (1977) Organization and functional meaning of dark-adopted receptive fields in the cat visual cortex. *Z. Vyssh. Nervn. Dejat.* **27,** 1159–1165 [in Russian].
30. Shevelev I. A., Volgushev M. A. and Sharaev G. A. (1983) Characteristics of dynamical reorganization of receptive fields of visual neurons under changes of light stimulation parameters. *Neurophysiologia, Kiev* **15,** 339–346 [in Russian].
31. Sillito A. M. (1979) Inhibitory mechanisms influencing complex cell orientation selectivity and their modification at high resting discharge levels. *J. Physiol., Lond.* **289,** 33–53.
32. Sillito A. M. (1985) Inhibitory circuits and orientation selectivity in the visual cortex. In *Models of the Visual Cortex* (eds Rose D. and Dobson V. G.), pp. 396–400. John Wiley, Chichester.
33. Verderevskaya N. N. and Shevelev I. A. (1982) Receptive fields of neurons in the cat's visual cortex after a change of alertness level. *Acta neurobiol. exp.* **42,** 75–92.
34. Volgushev M. A. (1989) Intracortical inhibition and adaptive reorganizations of receptive fields of neurons of the visual cortex. *Dokl. Acad. Nauk SSSR* **309,** 1483–1486 [in Russian].
35. Volgushev M. A., Shevelev I. A., Dec K., Sharaev G. A. and Verderevskaya N. N. (1983) Differences in dynamics of visual receptive field and its summation zone in cat. *Neurophysiologia, Kiev* **15,** 466–473 [in Russian].
36. Watanabe J., Fuse F., Inami T. and Iwai E. (1990) Spatiotemporal receptive field analysis of visual cortical neurons in awake monkey with random pattern stimuli. In *Vision, Memory and the Temporal Lobe* (eds Iwai E. and Mishkin M.), pp. 331–335. Elsevier, New York.
37. Yasui S., Davis W. and Naka K.-I. (1979) Spatio-temporal receptive field measurement of retinal neurons by random pattern stimulation and cross correlation. *IEEE Trans. biomed. Engng* **26,** 263–272.

(*Accepted* 8 *June* 1992)